

Characterization of Aqueous Plutonium(IV) Nitrate Complexes by Extended X-ray Absorption Fine Structure Spectroscopy

P. G. Allen,[†] D. K. Veirs,* S. D. Conradson,[‡] C. A. Smith, and S. F. Marsh

Nuclear Materials Technology Division and Materials Science and Technology Division, Los Alamos National Laboratory, Los Alamos, New Mexico 87545, and Glenn T. Seaborg Institute for Transactinium Science, Lawrence Livermore National Laboratory, Livermore, California 94551

Received August 24, 1995[⊗]

The structures of the aqueous nitrate complexes of Pu(IV) have been studied by extended X-ray absorption fine-structure (EXAFS) at nitric acid concentrations of 3, 8, and 13 M. Systematic changes in the EXAFS spectra demonstrate the trends of increasing nitrate ligation and decreasing water ligation as a function of increasing nitric acid concentration. The coordination numbers of the nitrogens and noncoordinating oxygens are consistent with previous studies in which the principal species were found to be the di-, tetra-, and hexanitrate complexes in these solutions. The Pu(IV) nitrate complexes in nitric acid appear to have similar actinide–nitrate structures as seen in the solid state structures of analogous thorium and neptunium nitrate compounds in which the nitrate ligands are planar and bidentate, and the central actinide atom is in the plane of the nitrates. The nitrates are distorted with respect to free nitrate in that the nitrogen–oxygen bond length of the noncoordinating oxygen is significantly shorter than the nitrogen–oxygen bond lengths of the coordinated oxygens. The plutonium in these complexes is highly coordinated with coordination numbers of 11–12 for the first shell of oxygen nearest neighbors. The average plutonium–oxygen (nitrate) bond length is 2.49 Å, and the average plutonium–oxygen (water) bond length is estimated to be 2.38 Å.

Introduction

Aqueous plutonium nitrate complexes are fundamental to the separation techniques presently employed to process nuclear materials. In the Purex process, an extractant composed of 30% TBP (tri-*n*-butyl phosphate) dissolved in a hydrocarbon diluent (dodecane or kerosene) is used to extract a Pu(IV) nitrate species from a complex mixture of fission products dissolved in concentrated nitric acid.¹ In anion exchange processes, a Pu(IV) nitrate complex is sorbed from 8 M nitric acid onto an anion exchange resin and washed off using 3 M nitric acid. Understanding the speciation of the Pu(IV) ion in nitric acid solutions is fundamental to understanding these processes and may lead to more efficient means of processing of nuclear materials. Increased processing efficiencies are important not only to reducing the volume of waste produced in ongoing separation processes, but also in separation processes that will be part of environmental remediation efforts. Despite their relevance to plutonium separation technologies and to the current multibillion dollar environmental restoration industry, the structures of plutonium nitrate complexes in solution have not been characterized.

The coordination chemistry of Pu(IV) nitrate complexes in solution has been studied extensively.^{2–10} For nitric acid

concentrations of 1–13 M, the extent of nitrate coordination increases as the nitric acid concentration increases. X-ray analysis has shown that the solid compounds (NH₄)₂Ce(NO₃)₆, (NH₄)₂Th(NO₃)₆, and (NH₄)₂Pu(NO₃)₆ are isomorphous.² The crystal structure of (NH₄)₂Ce(NO₃)₆ has been determined, and the hexanitratocerate anion was found to have six nitrate ligands each in bidentate coordination to the central cerium ion.¹¹ The visible absorption spectrum of Pu(IV) in 13 M nitric acid is essentially identical to the visible absorption spectra of both [(C₂H₅)₄N]₂Pu(NO₃)₆ and the tetrabutylammonium salt of Pu(IV) dissolved in various noncomplexing organic solvents.^{2,10} Thus, the principal Pu species in 13 M nitric acid is the hexanitrate anion with all of the nitrates complexed in bidentate geometry.

At nitric acid concentrations of 3 M, the principal species has been identified as Pu(NO₃)₂²⁺, extrapolating from detailed equilibrium data obtained from visible absorption spectroscopy.¹² Using stability constants of $\beta_1 = 3.9$ and $\beta_2 = 11.9$, the relative concentration of the mononitrate complex to the dinitrate complex is calculated to be 10%.¹³ The speciation in 8 M nitric acid is more complex and has been shown by absorption spectroscopy to contain at least one additional species along with the di- and hexanitrate complexes.¹⁴ The determination of this unknown species is important because the intensity

* To whom correspondence should be addressed at Nuclear Materials Technology Division, Los Alamos, National Laboratory.

[†] Lawrence Livermore National Laboratory.

[‡] Materials Science and Technology Division, Los Alamos National Laboratory.

[⊗] Abstract published in *Advance ACS Abstracts*, April 15, 1996.

- (1) (a) MacToth, L.; Bond, W. D.; Avens, L. R. *J. Met.* **1993**, 45-2, 35. (b) Cotton, F. A.; Wilkinson, G. *Advanced Inorganic Chemistry*, 5th ed.; John Wiley & Sons, Inc., New York, 1988; p 1010.
- (2) Hindman, J. C. in *The Transuranium Elements*, Seaborg, G. T., Katz, J. J., Manning, W. M., eds.; McGraw-Hill: New York, 1949; p 388.
- (3) Lahr, V. H.; Knock, W. *Radiochim. Acta* **1970**, 13, 1.
- (4) Grenthe, I.; Noren, B. *Acta Chem. Scand.* **1960**, 14, 2216.
- (5) Danesi, P. R.; Orlandini, F.; Scibona, G. *J. Inorg. Nucl. Chem.* **1966**, 28, 1047.

(6) Laxminarayanan, T. S.; Patil, S. K.; Sharma, H. D. *J. Inorg. Nucl. Chem.* **1964**, 26, 1001.

(7) Nitsche, H. *Mater. Res. Soc. Symp. Proc.* **1991**, 212, 517.

(8) Casellato, U.; Vigato, P. A.; Vidali, M. *Coord. Chem. Rev.* **1981**, 36, 183.

(9) Addison, C. C.; Logan, N.; Wallwork, S. C.; Garner, C. D. *Q. Rev., Chem. Soc.* **1971**, 25, 289.

(10) Ryan, J. R. *J. Phys. Chem.* **1960**, 64, 1375.

(11) Beineke, T. A.; Delgado, J. *Inorg. Chem.* **1968**, 7, 715.

(12) Veirs, D. K.; Smith, C. A.; Berg, J. M.; Zwick, B. D.; Marsh, S. F.; Allen, P. G.; Conradson, S. D. *J. Alloys Compds.* **1994**, 213/214, 328.

(13) Stability constants are derived from the 2.34 M data reported in ref 12. These are the best values at present. Experiments to obtain stability constants across a range of ionic strength are in progress.

Table 1. Selected Bond Lengths and Angles for Actinide Nitrate Complexes^a

compound	bond lengths (Å)					angles (deg)			ref
	<i>a</i>	<i>b</i>	<i>r</i> ₁	<i>r</i> ₂	<i>r</i> ₃	1	2	3	
Th(NO ₃) ₄ (H ₂ O) ₃ ·2H ₂ O									
NO ₃ (1)	2.50	2.62	1.27	1.28	1.21	124.0	121.5	114.5	16a
NO ₃ (2)	2.58	2.59	1.27	1.27	1.24	123.1	120.4	116.5	
Th(NO ₃) ₄ (H ₂ O) ₃ ·2H ₂ O									16b
NO ₃ (1)	2.53	2.62	1.27	1.25	1.20	123.2	121.7	115.2	
NO ₃ (2)	2.55	2.57	1.28	1.27	1.21	123.0	122.5	114.5	
[(H ₃ O)(I _a) ₂][Th(NO ₃) ₆]									17
NO ₃ (1,4)	2.55	2.56	1.30	1.28	1.21	123.9	121.5	114.6	
NO ₃ (2,5)	2.55	2.57	1.26	1.27	1.22	122.7	120.8	116.4	
NO ₃ (3,6)	2.58	2.59	1.27	1.28	1.20	123.5	121.8	114.6	
(4,4'-H _{1.5} bpy) ₂ (NO ₃) ₂ [Th(NO ₃) ₆]									18
NO ₃ (1)	2.58	2.58	1.26	1.27	1.23	121.6	121.2	117.0	
NO ₃ (2)	2.59	2.59	1.26	1.28	1.21	122.9	122.1	115.0	
NO ₃ (3)	2.52	2.56	1.29	1.27	1.21	121.1	122.4	116.4	
NO ₃ (4)	2.57	2.58	1.26	1.29	1.23	122.8	121.3	115.8	
NO ₃ (5)	2.58	2.60	1.26	1.28	1.23	123.4	119.8	116.8	
NO ₃ (6)	2.56	2.58	1.26	1.26	1.22	121.1	121.3	117.6	
(2,2'-H ₂ bpy) ₂ (NO ₃) ₂ [Np(NO ₃) ₆]·2H ₂ O									19
NO ₃ (1,4)	2.48	2.53	1.25	1.28	1.20	123.6	121.9	114.5	
NO ₃ (2,5)	2.50	2.51	1.27	1.27	1.21	122.8	122.5	114.8	
NO ₃ (3,6)	2.48	2.53	1.27	1.28	1.20	122.3	123.1	114.6	
(2,2'-H ₂ bpy)[Np(NO ₃) ₆]·2H ₂ O									20
NO ₃ (1)	2.46	2.50	1.30	1.26	1.20	122.0	125.0	113.4	
NO ₃ (2)	2.50	2.53	1.26	1.29	1.21	123.4	121.6	115.0	
NO ₃ (3)	2.48	2.49	1.28	1.26	1.21	122.0	122.6	115.4	
NO ₃ (4)	2.51	2.54	1.28	1.27	1.21	120.8	123.3	116.0	
NO ₃ (5)	2.51	2.54	1.27	1.27	1.22	122.9	121.0	116.0	
NO ₃ (6)	2.49	2.53	1.29	1.25	1.22	121.0	122.7	116.3	
[Pu(NO ₃) ₆] ²⁻	2.45	2.56	1.25	1.25	1.19	123.6	123.6	112.8	

^a I_a = (dicyclohexano-18-crown-6 isomer A). ^b bpy = bipyridyl.

of its visible absorption peak follows the sorption of Pu(IV) onto anion exchange resin, and as a result it may represent the complex involved in the sorption process. On the basis of NMR investigations from analogous Th complexes, the 8 M species has been tentatively assigned as Pu(NO₃)₄.¹² In the range of 3–13 M nitric acid concentrations, the tri- and pentanitrate Pu(IV) complexes have not yet been identified.

No complete structural determinations of single crystals containing the plutonium hexanitrate anion have been made to date, even though X-ray diffraction data have been reported for plutonium hexanitrate and tetranitrate salts.^{10,15} In contrast, several analogous thorium and neptunium nitrate compounds containing a central tetranitrate or hexanitrate cluster have been structurally characterized in the solid state.^{16–20} Table 1 lists crystallographically determined structural parameters for all of the Th and Np nitrate compounds that have been reported; the bond lengths and angles in Table 1 are labeled the same as the dimensions diagrammed in Figure 1. In these compounds, each nitrate group is rotated about the N atom such that the bidentate ligation is asymmetric and two different first shell An–O bond

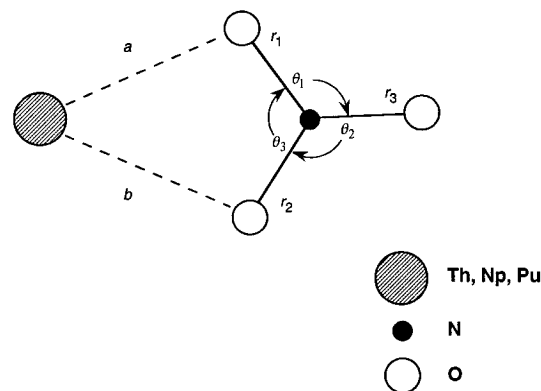


Figure 1. Diagram of bonding geometry showing bond lengths and angles for a bidentate nitrate bonded to a metal.

lengths (*a* and *b*) arise. The Np–O bond lengths *a* and *b* are shorter than those in the Th structures due to the actinide contraction in ionic radii. In each case, the structure of the bound nitrate is perturbed from that of free nitrate with the bond distance of the N to the noncoordinating O (*r*₃) being significantly shorter than the N–O bond distances to the coordinating oxygens (*r*₁ and *r*₂). The hexanitrate anions from the compounds in ref 17–19 can be depicted by icosahedron with near-*T_h* symmetry. The Np(NO₃)₆²⁻ central anion as determined in ref 20 is a more distorted icosahedron.

In the present study, we describe the results of an extended X-ray absorption fine-structure (EXAFS) study on the nitrate complexes of Pu(IV) as a function of varying nitric acid concentration. The distances from the plutonium ion to shells of nearest neighbors and the numbers of atoms in the nearest-neighbor shells are determined. From this information the plutonium coordination number for different nitrate complexes and the average plutonium–nitrate structure can be inferred.

- (14) Marsh, S. F.; Day, R. S.; Veirs, D. K. Spectrophotometric Investigations of the Pu(IV) Nitrate Complex Sorbed by Ion Exchange Resins. Report LA-12070; Los Alamos National Laboratory: Los Alamos, NM, June 1991.
- (15) Staritsky, E. *Anal. Chem.* **1956**, *28*, 2021.
- (16) (a) Ueki, T.; Zalkin, A.; Templeton, D. H. *Acta Crystallogr.* **1966**, *20*, 836. (b) Taylor, J. C.; Mueller, M. H.; Hitterman, R. L. *Acta Crystallogr.* **1966**, *20*, 842.
- (17) Ming, W.; Boyi, W.; Peiju, Z.; Wenji, W.; Jie, L. *Acta Crystallogr.* **1988**, *C44*, 1913.
- (18) Rammo, N. N.; Hamid, K. R.; Khaleel, B. A. *J. Less Common Met.* **1990**, *162*, 1.
- (19) Grigor'ev, M. S.; Gulev, B. F.; Krot, N. N. *Radiokhimiya* **1986**, *28*, 685.
- (20) Grigor'ev, M. S.; Yanovskii, A. I.; Krot, N. N. *Radiokhimiya* **1987**, *29*, 574.

Experimental Section

Cell and Solution Preparation. The cells used in this study had to be designed to enable EXAFS studies of Pu (principally ^{239}Pu) in concentrated nitric acid solution at a nonnuclear facility. As a result, there were several important design criteria that addressed safety concerns as well as experimental requirements. The criteria were as follows: (1) three levels of sample containment as a precaution against any release of Pu into the surrounding environment; (2) *in-situ* mechanism for mixing solutions immediately prior to EXAFS data acquisition in order to minimize radiolysis effects such as disproportionation or introduction of fluoride ion into solution from the Teflon inner window; and (3) X-ray transparent, acid resistant windows on each level of sample containment to permit spectra acquisition and maintain containment.

The primary sample cell consisted of a Kynar body with one Teflon window and one polyethylene window attached to a plunger assembly with a reservoir for nitric acid. This cell was placed in a second Kynar container with Kapton windows (Kynar is a polyvinylidene fluoride material available from Elf Atochem; Kapton is a high-strength polyimide film available from DuPont; Teflon is a polytetrafluoroethylene polymer available as a film from DuPont). A 30 μL aliquot of plutonium stock solution (0.837 M Pu in 7 M nitric acid) was allowed to dry on the inner Teflon window and a 0.5 mL aliquot of the appropriate acid was placed in the reservoir (3, 8, or 13 M nitric acid). The primary cell was assembled, decontaminated if necessary to less than 20 disintegrations per minute (dpm) removable contamination and less than 100 dpm fixed contamination, and placed in the second container. No detectable contamination was on the secondary container; the detection limit was less than 20 dpm. At the moment just prior to EXAFS data acquisition, the nitric acid was introduced into the sample chamber, dissolving the plutonium nitrate salt and yielding a final solution of 0.05 M Pu (or 12 g/l) in 3, 8, or 13 M nitric acid (due to inefficiencies in transferring the nitric acid, the final Pu concentration may have been higher). This assembly was then sealed in a third container with Kapton windows which was mounted in the X-ray experimental hut.

EXAFS Data Acquisition and Analysis. Plutonium L_{III} -edge X-ray absorption spectra were collected at the Stanford Synchrotron Radiation Laboratory on wiggler beam line 4-2 (unfocused) under dedicated ring conditions (3.0 GeV, 50–100 mA) using a Si (220) double-crystal monochromator. Rejection of higher-order harmonic content in the beam was achieved by employing a flat Rh-coated quartz mirror tuned at a critical angle for the rejection of photons having energies above 22 000 eV. Having rejected greater than 95% of the higher order harmonics with the mirror, the monochromator was operated fully tuned with respect to θ , the orientation between the two crystals. Spectra were collected in transmission mode using three N_2 -filled ionization chamber detectors and a vertical slit height of 1 mm. The path length of the cells was designed (based on a Pu concentration of 0.05 M) so that an edge jump of ~ 1 absorption unit was achieved over the L_{III} absorption edge at 18056 eV. Data reduction and analysis were performed using techniques previously reported.²¹ Three EXAFS scans were collected on each solution at ambient temperature ($\sim 25^\circ\text{C}$) and averaged to improve the statistics. The spectra were energy calibrated by simultaneously measuring the spectrum of a Zr foil which was placed between the second and third ion chambers, defining the first inflection point at the Zr K-edge as 17998 eV. The data were normalized by setting the edge jump equal to unity at the ionization threshold, defined as 18080 eV. A four-region spline function was used to fit the background over the EXAFS region which extended out to $k = 15 \text{ \AA}^{-1}$. Fourier transforms of the k^3 -weighted data were calculated over the range $k = 2.4\text{--}14.4 \text{ \AA}^{-1}$ with a Gaussian window function of 0.2 \AA^{-1} half-width. Back transforms were done from $R = 1.0\text{--}4.2 \text{ \AA}$ using a Gaussian window function with half-width of 0.05 \AA . Curve-fitting was done on this Fourier-filtered EXAFS data over the range $k = 3\text{--}14 \text{ \AA}^{-1}$. Theoretical phases and amplitudes derived from the program

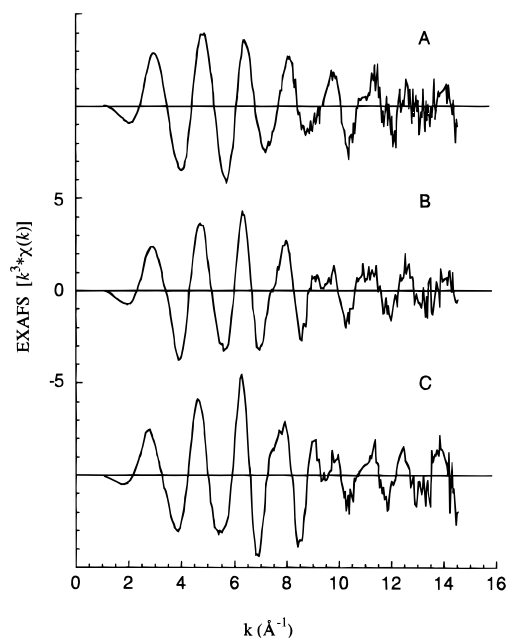


Figure 2. Background subtracted k^3 -weighted EXAFS spectra of the Pu (IV) ion in solution with nitric acid concentrations of (A) 3 M, (B) 8 M, and (C) 13 M.

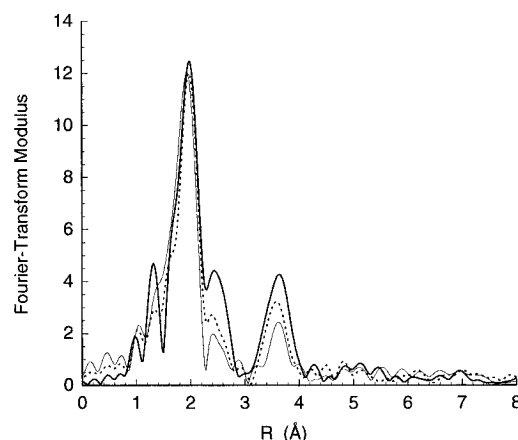


Figure 3. Comparison of the Fourier transforms of EXAFS data ($k = 2.4\text{--}14.4 \text{ \AA}^{-1}$) from Pu (IV) in 3 M (thin solid line), 8 M (dashed line), and 13 M nitric acid (thick solid line).

FEFF were used to fit the contributions from the O and N neighbors.²² All fits included contributions from the first shell of directly coordinated O atoms (from the nitrate and water ligands), the second shell of nitrate N atoms, and the third shell of noncoordinating nitrate O atoms. For each fit, only the bond lengths (R) and coordination numbers (N) were allowed to vary.

Results and Discussion

Figure 2 shows the raw k^3 -weighted EXAFS data for each solution, demonstrating the data quality and relative noise levels over the entire k -range. Although the spectra are quite similar at this level of analysis, there are noticeable differences. The 3 M spectrum is dominated by a single frequency oscillation. The 8 and 13 M spectra show the presence of a beat at $k = 9 \text{ \AA}^{-1}$, and the amplitude envelope in the EXAFS data becomes more complex.

The Fourier transforms of the k^3 -weighted raw EXAFS data (Figure 3) reveal the relative position and the relative number of nearest neighbors of Pu in concentrated nitric acid. The peaks

(21) Prins, R.; Koningsberger, D. C. *X-ray Absorption: Principles, Applications, Techniques for EXAFS, SEXAFS, and XANES*; Wiley: New York, 1988.

(22) Rehr, J. J.; Mustre de Leon, J.; Zabinsky, S.; Albers, R. C. *Phys. Rev. B* **1991**, *44*, 4146.

Table 2. Summary of EXAFS Curve-Fitting Results^{a,b}

acid concn (M)	inner O shell		inner O shell		N shell		outer O shell	
	N	R, Å	N	R, Å	N	R, Å	N	R, Å
3	11.1	2.41			2.6	2.96	2.9	4.14
8	10.8	2.45			4.0	2.97	4.3	4.15
13	12.0	2.49			6.0	2.97	6.0	4.16
	6.0	2.45	6.0	2.56	6.0	2.97	6.0	4.16

^a Errors in distances (± 0.02 Å) and coordination numbers ($\pm 15\%$) are estimated from the deviation between fitting results from models of known structure and their true values. ^b Relative coordination numbers were obtained by normalization with respect to those for the 13 M nitric acid sample which is known to be $\text{Pu}(\text{NO}_3)_6^{2-}$.

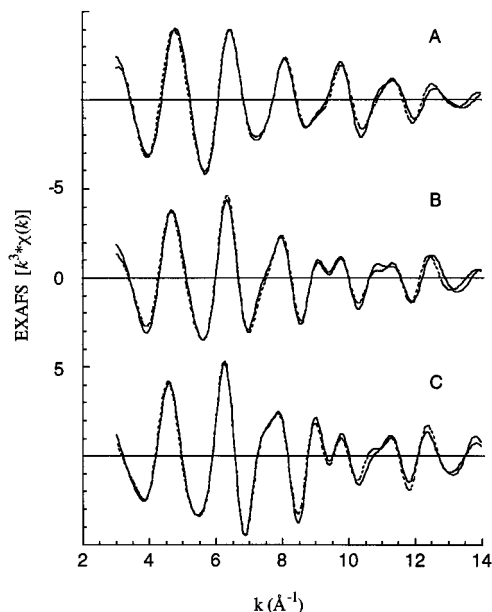


Figure 4. Nonlinear least-squares curve-fits (---) to the Fourier filtered EXAFS data (—) of Pu(IV) in solution with nitric acid concentrations of (A) 3 M, (B) 8 M, and (C) 13 M.

are shifted to lower R due to the EXAFS phase shift, $\alpha = 0.2$ – 0.5 Å. The largest peak at 2.0 Å represents contributions from nearest neighbor O atoms arising from the nitrate and water ligands. The peaks at 2.5 and 3.7 Å arise from the N and noncoordinating O of the nitrate species and reflect the relative number of nitrates bound to Pu. The relative distances from the first shell oxygens to the second shell nitrogens is 0.5 Å and the relative distance from the second shell nitrogens to the third shell oxygens is 1.2 Å. These distances are entirely consistent with the bidentate geometry in Figure 1 and are not consistent with a unidentate structure. Systematic increases in the intensities of the second-shell nitrogen and the third-shell, noncoordinating oxygen peaks clearly demonstrate the trend of increasing nitrate ligation as a function of increasing nitric acid concentration. At the same time the number of first shell oxygens do not appear to change substantially with increasing nitric acid concentration, indicating that the nitrates are replacing the inner coordination-shell water and the overall plutonium coordination number is left relatively unchanged.

The results of curve-fitting spectra from the 3, 8, and 13 M nitric acid solutions are summarized in Table 2. A comparison between EXAFS data calculated from the curve fits and the Fourier-filtered experimental data is shown in Figure 4. The fit of the 13 M nitric acid solution data yielded ratios of the number of oxygen atoms in the first shell to the number of nitrogen atoms in the second shell to the number of oxygen atoms in the third shell of approximately 2:1:1. In addition, the distances between shells are consistent with the bidentate

structure. Therefore, the coordination numbers determined for the three solutions and reported in Table 2 have been normalized so that the coordination numbers in 13 M nitric acid are 12.0, 6.0, and 6.0, respectively, reflecting the fact that this species is $\text{Pu}(\text{NO}_3)_6^{2-}$.

We will now discuss the results for the 13 M case in which the species is clearly the hexanitrate complex. The average Th–O(nitrate) distances for the two compounds in Table 1 containing a central thorium hexanitrate moiety is 2.57 Å and the average Np–O(nitrate) distance for the two compounds in Table 1 containing a central neptunium hexanitrate moiety is 2.51 Å. These distances can be compared to the average Pu–O(nitrate) distance determined here of 2.49 Å (Table 2) by noting that the ionic radii of the Th, Np, and Pu are 0.94 , 0.87 , and 0.86 Å, respectively.²³ The differences between the Pu–O (nitrate) average distance and the Th,Np–O distances of 0.08 and 0.02 Å are in excellent agreement with the differences between the Pu ionic radius and Th,Np ionic radii of 0.08 and 0.01 Å. A fit of the 13 M solution EXAFS data using two first shell oxygen distances improved the quality of fit by 30% and gave 6 O at 2.45 Å and 6 O at 2.56 Å (last line of Table 2). The difference in these Pu–O distances is consistent with, but slightly larger than, the difference between the two An–O distances reported for the four solid compounds. This difference arises from a rotation of the nitrate ligand about the central nitrogen atom. The average distance between the nitrogen and the noncoordinating oxygen for the four solid compounds in Table 1 that contain a central hexanitrate moiety is 1.21 Å. The difference between the second shell nitrogen distance (2.97 Å) and the third shell oxygen distance (4.15 Å) is 1.18 Å, in agreement with the solid compound data. Using the bond lengths obtained for the 13 M solution and assuming that the nitrate is planar with the plutonium ion contained within the plane of the nitrate and that the N–O bond lengths (r_1 and r_2) are 1.25 Å, the nitrate bond angles were calculated. This result appears in Table 1 for comparison. The agreement with the values for the solid compounds for all distances and angles strongly suggests that the assumptions just mentioned are correct.

We will now discuss the results of fitting the EXAFS data for the 8 and 3 M nitric acid solutions reported in Table 2. In the 8 and 3 M solutions there are 11 O atoms at 2.45 and 2.41 Å, respectively. The numbers of N and noncoordinating O atoms for the 8 M solution, 4.2, and the 3 M solution, 2.8, are consistent with a mixture of the dinitrato, tetranitrato, and hexanitrate species in the 8 M nitric acid solution and a mixture of the dinitrato and tetranitrato species in the 3 M nitric acid solution as reported previously.^{12,24} Taken together, these results suggest that the hydration number for the tetranitrato species is 3 and for the dinitrato species it is 7. Since the Th–O (water) distances in $\text{Th}(\text{NO}_3)_4(\text{H}_2\text{O})_3 \cdot 2\text{H}_2\text{O}$ (2.41 – 2.48 Å)¹⁶ are considerably shorter than the Th–O(nitrate) distances of 2.57 Å, the corresponding Pu–O(water) distances should range from 2.34 to 2.41 Å based on differences in the ionic radii. However, because the resolution in EXAFS is limited by $\Delta R \sim \pi/2k_{\text{max}}$ (0.11 Å for these results) and since there are multiple distances for the nitrate and water oxygens, it is difficult to separate these contributions. In spite of this, the observed bond length contraction for the first shell of O atoms and the lack of any significant movement of the nitrate ligands relative to the 13 M data (N and noncoordinating O remain fixed) indicate that a

(23) Seaborg, G. T. *Radiochim. Acta*, **1993**, *61*, 115.

(24) Because XAFS results are based on an average structure, a equimolar mixture of $\text{Pu}(\text{NO}_3)_6^{2-}$, $\text{Pu}(\text{NO}_3)_2(\text{H}_2\text{O})_7^{2+}$ and $\text{Pu}(\text{NO}_3)_4(\text{H}_2\text{O})_3$ should be indistinguishable from a solution containing only $\text{Pu}(\text{NO}_3)_4(\text{H}_2\text{O})_3$, provided that the orientations of the nitrate and water ligands are independent of their coordination numbers.

model of increasing hydration numbers with shorter Pu–O (water) distances is appropriate. In such a model, the tetranitrato complex would have eight Pu–O(nitrate) bonds with distances of 2.49 Å and three Pu–O(water) bonds with distances of 2.38 Å (we use the average Pu–O(nitrate) bond distance of 2.49 Å from these results for the hexanitrato complex where there is no complicating waters present and a Pu–O(water) bond distance of 2.38 Å derived from the Th compounds). The average of these bond lengths for the tetranitrato species is 2.46 Å. The dinitrato complex would have four Pu–O(nitrate) bonds and seven Pu–O(water) bonds, yielding an average Pu–O distance of 2.42 Å. Thus, the observation of contraction in the first shell oxygen distances as the nitric acid concentration decreases can be explained by a model in which the distance between the plutonium atom and the water oxygen is shorter than the distance between the plutonium atom and nitrate oxygen.

Conclusion

The Pu(IV) nitrate complexes in nitric acid have similar plutonium–nitrate structures to those seen in solid analogues.

Our results suggest that the nitrate ligands are planar and bidentate. The nitrate is distorted in a manner similar to that in the solid compounds with the N–O bond length of the noncoordinating oxygen being significantly shorter than the coordinating N–O bond lengths. For the hexanitrato complex there appears to be a slight rotation of the nitrate about the central nitrogen atom. The Pu(IV) is highly coordinated with coordination numbers of 11–12 for the first shell of O nearest neighbors. The average Pu–O bond length for the water ligand is shorter than the average Pu–O bond length for the nitrate ligand.

Acknowledgment. The EXAFS data were obtained at SSRL which is operated by the Department of Energy, Division of Chemical Sciences. This work was funded by the US Department of Energy under Contract W-7405-ENG-36 and the Defense Advanced Research Projects Agency.

IC9511231